

A functional single-molecule binding assay via force spectroscopy

Yi Cao, M. M. Balamurali, Deepak Sharma, and Hongbin Li*

Department of Chemistry, University of British Columbia, Vancouver, BC, Canada V6T 1Z1

Edited by James A. Spudich, Stanford University School of Medicine, Stanford, CA, and approved August 24, 2007 (received for review June 7, 2007)

Protein–ligand interactions, including protein–protein interactions, are ubiquitously essential in biological processes and also have important applications in biotechnology. A wide range of methodologies have been developed for quantitative analysis of protein–ligand interactions. However, most of them do not report direct functional/structural consequence of ligand binding. Instead they only detect the change of physical properties, such as fluorescence and refractive index, because of the colocalization of protein and ligand, and are susceptible to false positives. Thus, important information about the functional state of protein–ligand complexes cannot be obtained directly. Here we report a functional single-molecule binding assay that uses force spectroscopy to directly probe the functional consequence of ligand binding and report the functional state of protein–ligand complexes. As a proof of principle, we used protein G and the Fc fragment of IgG as a model system in this study. Binding of Fc to protein G does not induce major structural changes in protein G but results in significant enhancement of its mechanical stability. Using mechanical stability of protein G as an intrinsic functional reporter, we directly distinguished and quantified Fc-bound and Fc-free forms of protein G on a single-molecule basis and accurately determined their dissociation constant. This single-molecule functional binding assay is label-free, nearly background-free, and can detect functional heterogeneity, if any, among protein–ligand interactions. This methodology opens up avenues for studying protein–ligand interactions in a functional context, and we anticipate that it will find broad application in diverse protein–ligand systems.

atomic force microscopy | protein–ligand binding | protein–protein interaction

Protein–ligand interactions, including protein–protein interactions, play crucial roles in almost all biological processes and functions and have important applications in medicine and biotechnology (1). The binding of a ligand to the protein will induce conformational change of the protein, which can be a minute structural perturbation or a large conformation change, and transform the protein into a new functional state that is distinct from the ligand-free form of the protein. This new functional state then can trigger a cascade of biological reactions (2, 3). Many techniques have been developed to characterize protein–ligand interactions and measure their binding affinity *in vitro* and *in vivo* (4–6). However, most of the techniques are largely based on colocalization of the proteins and their interacting partners and involve the detection of change of physical properties upon binding of the ligand, such as fluorescence and refractive index, which are not necessarily the structural or functional consequence of ligand binding. However, the functional protein–ligand complexes (ligand-bound functional states) are not merely the colocalization of the two interacting partners. Instead, it is the structural difference, being minute or large, and its functional consequence that distinguish the functional ligand-bound form from the nonfunctional ligand-free form. Hence, it is of critical importance to probe the structural and/or functional consequence of the protein upon binding of ligands and develop functional binding assay to directly report the functional state of the protein–ligand complex.

Mechanical stability is an intrinsic property of a given protein and is governed by specific noncovalent interactions in the key region of the protein (7–9). As such, mechanical stability is susceptible to conformational changes of the proteins caused by external factors, such as ligand binding (10) and point mutation (11). Mechanical stability of proteins can be directly measured using single-molecule atomic force microscopy (AFM) one molecule at a time (7, 12). Therefore, if ligand binding can induce conformational changes in the protein to alter its mechanical stability, mechanical stability of the protein then can serve as an intrinsic reporter to directly report the structural consequence of ligand binding to the protein, thus entailing a functional means to directly identify the functional state of the protein at the single-molecule level without any ambiguity. As a proof of principle, here we use the binding of Fc fragment of human IgG (hFc) to protein G as a model system (13) to report a force-spectroscopy-based, functional single-molecule binding assay that is capable of directly reporting the functional state of protein G upon binding of hFc. In this assay, the mechanical stability of protein G is used as a functional reporter to directly report the functional/structural consequence of the binding of hFc to protein G.

Protein G from streptococci is well known for its ability to bind IgG antibody and has been used as affinity purification matrix for purifying IgG antibody (13, 14). The binding of hFc to protein G domains has been widely studied and used as a model system for a wide range of binding assays (15–19). Protein G contains three IgG binding domains (B1, C2, and B2 domains) arranged in tandem whose sequences only differ from each other by a few amino acid residues [supporting information (SI) Fig. 4]. All three IgG binding domains have similar structures, which are characterized by a four-strand β -sheet packed against an α -helix (SI Fig. 4), and are predicted to bind Fc in an almost identical fashion as C2 domain binds to Fc (20). The three-dimensional structure of Fc/C2 complex shows that Fc binds to C2 domain in the region of the C-terminal part of the α -helix, the N-terminal part of the third β -strand, and the loop between the two structural elements (20) and the binding does not introduce major structural change to protein G (20). The mechanical stability of B1 IgG binding domain (GB1) has been well characterized by using single-molecule AFM techniques (21, 22), and it was shown that its mechanical stability depends on the backbone hydrogen bonds in the β -sheet as well as hydrophobic interactions (23). Thus, we use GB1 and its mutant NuG2 (24)

Author contributions: H.L. designed research; Y.C., M.M.B., and D.S. performed research; Y.C. analyzed data; and Y.C. and H.L. wrote the paper.

The authors declare no conflict of interest.

This article is a PNAS Direct Submission.

Abbreviations: AFM, atomic force microscopy; hFc, Fc fragment of human IgG; wt, wild type; WLC, worm-like chain.

*To whom correspondence should be addressed. E-mail: hongbin@chem.ubc.ca.

This article contains supporting information online at www.pnas.org/cgi/content/full/0705367104/DC1.

© 2007 by The National Academy of Sciences of the USA

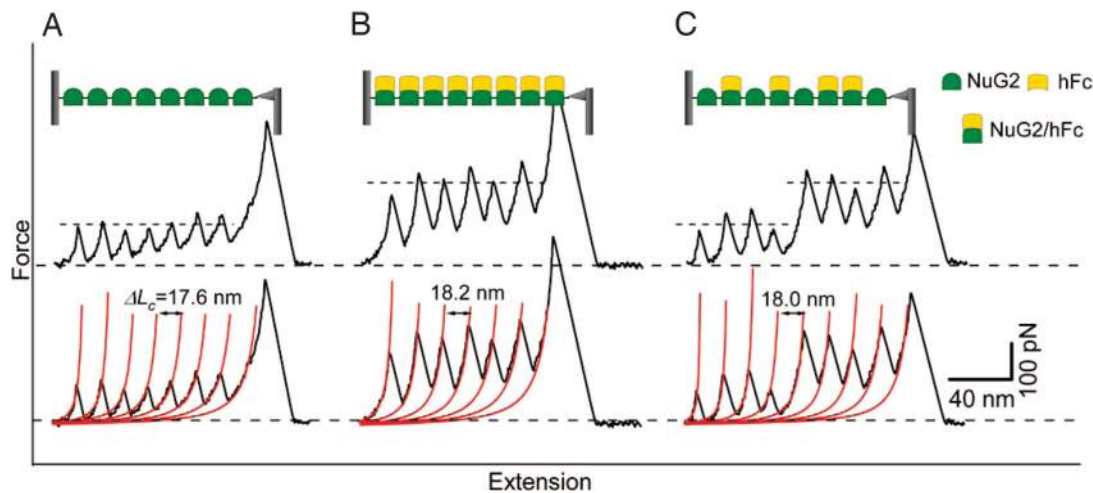


Fig. 1. Mechanical stability of NuG2 is a functional reporter for the binding of hFc. (A) Stretching polyprotein (NuG2)₈ results in typical sawtooth-like force–extension curves that are characterized by unfolding forces of ≈ 105 pN and contour length increments ΔL_c of ≈ 18 nm. Each individual force peak corresponds to the mechanical unfolding of individual NuG2 domains in the polyprotein. All of the NuG2 domains unfold at a similar force of ≈ 105 pN, as indicated by the dashed line. Red lines correspond to the WLC fits to the force–extension curve with ΔL_c of 17.6 nm. (B) The mechanical stability of NuG2 is enhanced by the binding of hFc. When preequilibrated with 33.3 μ M hFc, the majority of NuG2 domains unfold at much higher forces of ≈ 210 pN, indicating that the unfolding force of NuG2 can be used as an indicator to report effective hFc binding to NuG2. Red lines correspond to the WLC fits to the force–extension curve with ΔL_c of 18.2 nm. (C) Force–extension curves of NuG2 at an intermediate concentration of hFc directly identify the hFc-bound and hFc-free forms of NuG2 at the single-molecule level. When preequilibrated with 17.8 μ M hFc, the unfolding forces of NuG2 occur at two distinct levels (as indicated by the dashed lines): the first four unfolding events occurred at ≈ 105 pN and can be ascribed to the unfolding of hFc-free NuG2; the last four unfolding events occurred at ≈ 210 pN, which corresponds to the unfolding of hFc-bound NuG2. Red lines correspond to the WLC fits to the experimental data. (Insets) Schematic illustration of the stretching of (NuG2)₈ polyprotein between an AFM tip and glass substrate in the absence or presence of hFc. The functional states of NuG2 domains in the polyprotein also are indicated.

as models to demonstrate the feasibility of the force-spectroscopy-based single-molecule functional binding assay.

Results

Mechanical Stability of NuG2 Is Enhanced by the Binding of hFc. NuG2 is a GB1 mutant computationally designed by David Baker's group (University of Washington, Seattle, WA), and its three-dimensional structure is very similar to that of wild-type (wt)-GB1 (24). Although the three-dimensional structure of NuG2/hFc complex is not known, it is anticipated that the structure of NuG2/hFc will be very similar to that of wt-GB1/Fc. To characterize the mechanical stability of NuG2, we constructed a polyprotein (NuG2)₈, which is composed of eight identical tandem repeats of NuG2 domains. Stretching the polyprotein (NuG2)₈ results in force–extension relationships of characteristic sawtooth pattern appearance, where the individual sawtooth peak corresponds to the sequential mechanical unfolding event of individual NuG2 domains in the polyprotein chain (Fig. 1A). The unfolding force peaks are equally spaced. Fits of the worm-like chain (WLC) model of polymer elasticity (25) to the consecutive unfolding force peaks (red lines) measure a contour length increment (ΔL_c) of ≈ 18.0 nm for the mechanical unfolding of NuG2, in good agreement with the expected value for mechanical unfolding of NuG2. ΔL_c is an intrinsic structural property of a given protein (7) and serves as a fingerprint for us to identify the mechanical unfolding of NuG2. Because the NuG2 domains in the polyprotein chain are identical to each other, the mechanical unfolding of NuG2 domains occur at similar forces. The average unfolding force of NuG2 domains is 105 ± 20 pN (average \pm SD, $n = 1,773$) at a pulling speed of 400 nm/s (Fig. 2A).

Although the binding of hFc to NuG2 does not introduce major structural changes to NuG2, it enhances the mechanical stability of NuG2 significantly. Stretching (NuG2)₈ that is preequilibrated with 33 μ M hFc results in sawtooth-like force–extension curves. WLC fits to the consecutive force peaks

measure ΔL_c of ≈ 18 nm, indicating that the unfolding force peaks result from the mechanical unfolding of NuG2 domains. However, the majority of NuG2 domains unfold at a much higher average force of 210 ± 20 pN ($n = 223$) than that of NuG2 in the absence of hFc (Fig. 1B). Because the vast majority of the NuG2 domains are bound to Fc at this concentration of hFc, we attribute the higher unfolding force of 210 pN to the mechanical unfolding of the hFc-bound form of NuG2. Control experiments ruled out the possibility that the higher force peaks were caused by either the mechanical unfolding of Ig domains of hFc (SI Fig. 5) or the Tris/azide buffer used for hFc (SI Fig. 6). These results strongly indicate that the binding of hFc to NuG2 significantly reinforced the mechanical resistance of NuG2 to the force-induced unfolding, despite the small apparent structural changes caused by the binding of hFc.

Mechanical Stability of NuG2 Serves as a Functional Reporter for the Binding of hFc to NuG2. Because the hFc-bound form of NuG2 is mechanically distinct from that of hFc-free form of NuG2, it becomes possible to use the mechanical stability of NuG2 as a functional reporter to directly report the binding state of NuG2 domains one molecule at a time and determine the relative population of the two forms of NuG2 in the presence of hFc. Indeed, when carrying out single-molecule AFM experiments of NuG2 at various concentrations of hFc, we observed two distinct populations of NuG2. For example, stretching (NuG2)₈ preequilibrated with 17.8 μ M hFc resulted in force–extension curves with equally spaced unfolding force peaks but with two distinct levels of unfolding forces, one located at ≈ 105 pN and a second level at ≈ 210 pN. A typical force–extension curve is shown in Fig. 1C, where four unfolding events occurred at ≈ 105 pN and the other four occurred at ≈ 210 pN. The unfolding force histogram (Fig. 2E) shows two clearly separate unfolding force peaks centered at 105 pN and 210 pN, respectively. We can readily identify the NuG2 domains that unfold at ≈ 105 pN as the hFc-free form of NuG2, whereas the NuG2 domains unfold at

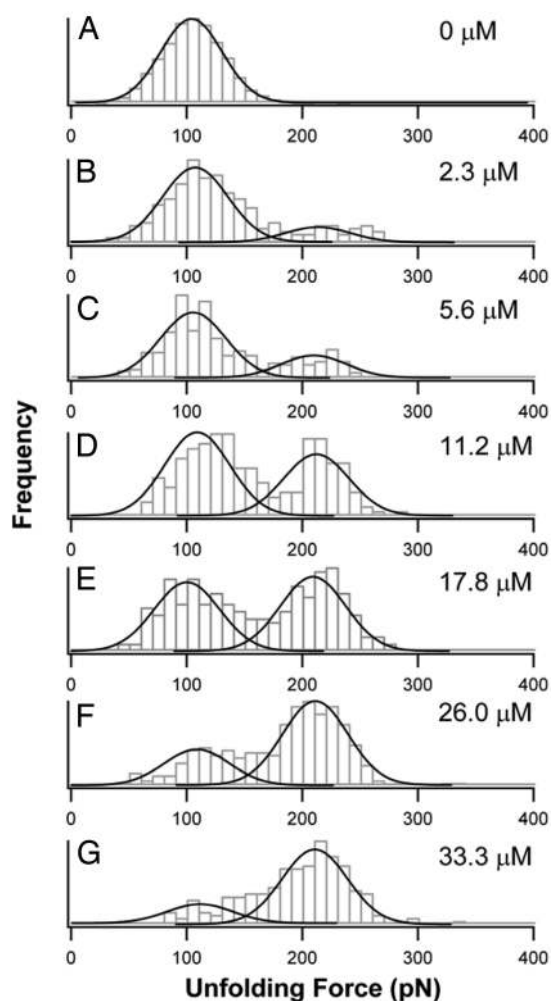


Fig. 2. Unfolding force histograms of NuG2 in the presence of hFc reveal two distinct populations of NuG2 (hFc-free and hFc-bound forms). (A) Unfolding force histogram of NuG2 in the absence of hFc. The solid line is a Gaussian fit to the experimental data. (B–G) Unfolding force histograms of NuG2 pre-equilibrated with different concentrations of hFc. The unfolding force histograms of NuG2 show two clear separate peaks in the presence of hFc: one is at 105 pN, which corresponds to the unfolding of hFc-free NuG2, and the other is at 210 pN, which corresponds to the unfolding of NuG2 in the complex with hFc. The initial concentration of hFc for each histogram is shown on the right. Each unfolding force histogram was fitted with two Gaussian functions (solid lines), and the relative areas underneath the Gaussian fits directly measure the fraction of hFc-free and hFc-bound of NuG2.

≈210 pN as the hFc-bound forms of NuG2. By counting the number of unfolding events of NuG2 occurring at low and high forces, we can readily determine the distribution of NuG2 among the two distinct populations: hFc-bound and hFc-free forms of NuG2.

By varying the concentration of hFc, we investigated the change of the distribution of the two forms of NuG2. The unfolding force histograms of NuG2 under different concentrations of hFc are shown in Fig. 2. It is evident that, in the presence of hFc, the unfolding force histograms of NuG2 show bimodal distribution, with one peak at ≈105 pN and a second one at ≈210 pN. As expected, upon increasing the concentration of hFc, more unfolding events occur at ≈210 pN and fewer unfolding events occur at ≈105 pN. And eventually the unfolding events at ≈210 pN become dominant. This result clearly demonstrates that the hFc-free NuG2 are converted to hFc-bound form of NuG2 upon increasing the concentration of hFc. The positions of the two

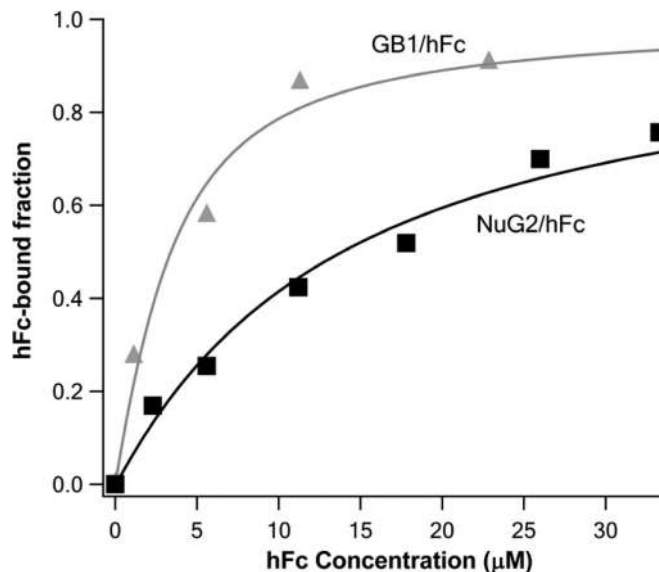


Fig. 3. Accurate determination of dissociation constant K_d using force-spectroscopy-based single-molecule binding assay. The fractions of hFc-bound NuG2 and wt-GB1 are plotted against the initial concentration of ligand hFc in the binding isotherm (squares, NuG2/hFc; triangles, wt-GB1/hFc). Solid lines are fits to the binding isotherms using a single binding site model that takes into account all of the species present in solution (black line, NuG2/hFc; gray line, wt-GB1/hFc). The measured K_d is $12.6 \pm 0.9 \mu\text{M}$ for the binding of hFc to NuG2 and $2.2 \pm 0.4 \mu\text{M}$ for the binding of hFc to wt-GB1.

unfolding force peaks in the histograms remain unchanged at different hFc concentrations, indicating that the mechanical stability of hFc-bound and hFc-free forms of NuG2 does not depend on hFc concentration, and hence the observed two populations of NuG2 reflect the two intrinsic functional states of NuG2 caused by the specific binding of hFc to NuG2.

Measuring the Dissociation Constant of hFc to NuG2 at the Single-Molecule Level. The fractions of hFc-bound and hFc-free NuG2 were determined directly from the relative areas under the peaks at 105 pN and 210 pN, respectively (Fig. 2). The fractions of hFc-bound NuG2 are plotted against hFc concentration (Fig. 3, squares). Because NuG2 domains in the polyprotein bind hFc in an independent fashion, as determined by surface plasmon resonance technique (data not shown), we fitted the binding isotherm to a single-site binding model, which takes into account all of the species present, and measured a dissociation constant K_d of $12.6 \pm 0.9 \mu\text{M}$ for the binding of hFc to NuG2.

To test the sensitivity of this method, we also studied the binding of hFc to wt-GB1. Similar to NuG2, the mechanical stability of GB1 increased significantly upon binding of hFc. The unfolding force of GB1 increased from 180 pN to 265 pN (data not shown). Following similar procedures, we measured the hFc-bound fraction of GB1 as a function of hFc concentration (Fig. 3, triangles) and determined K_d of $2.2 \pm 0.4 \mu\text{M}$ for the binding of GB1 to hFc. Although K_d for NuG2 and GB1 only differ by six times, the force-spectroscopy-based single-molecule binding assay readily detects this difference, demonstrating the high sensitivity of the single-molecule force spectroscopy-based binding assay. It is of note that, although K_d of NuG2 to hFc is approximately six times higher than that of GB1 to hFc, the stabilization effect on the mechanical stability upon binding of a ligand is similar in both cases. Therefore, the sensitivity of force spectroscopy does not depend on the binding strength between protein and its ligand.

However, it is worth noting that the sensitivity and accuracy

with polyprotein. The AFM experiments were carried out after allowing the mixture to equilibrate for ≈ 30 min. The results for these two mixing methods were identical. The spring constant of each individual cantilever [Si_3N_4 cantilevers from Veeco Probes

GB1, each unfolding force histogram was fitted with two Gaussian functions. The binding curves were fitted by using a single binding site model that takes into account all of the species present in solutions:

$$\text{Bound\%} = \frac{[\text{NuG2}]_0 + [\text{hFc}]_0 + K_d - \sqrt{([\text{NuG2}]_0 + [\text{hFc}]_0 + K_d)^2 - 4[\text{NuG2}]_0[\text{hFc}]_0}}{2[\text{NuG2}]_0},$$

(Camarillo, CA), with a typical spring constant of $15 \text{ pN}\cdot\text{nm}^{-1}$ was calibrated in PBS buffer by using the equipartition theorem before each experiment. The pulling speed used for all of the pulling experiments was $400 \text{ nm}\cdot\text{s}^{-1}$. The spacing between consecutive unfolding events was determined in an unbiased and hands-off fashion by using an algorithm custom-written in Igor Pro 5.0 (WaveMetrics, Lake Oswego, OR).

To estimate the fraction of hFc-bound NuG2 or hFc-bound

where $[\text{NuG2}]_0$ is the initial concentration of NuG2 domains in the solution, $[\text{hFc}]_0$ is the initial concentration of hFc in the solution, and K_d is the dissociation constant (37).

We thank David Baker for providing constructs containing proteins NuG2 and GB1. This work was supported by the Natural Sciences and Engineering Research Council of Canada, the Canada Research Chairs Program, and the Canada Foundation for Innovation.

1. Arkin MR, Wells JA (2004) *Nat Rev Drug Discovery* 3:301–317.
2. Swain JF, Gierasch LM (2006) *Curr Opin Struct Biol* 16:102–108.
3. Changeux JP, Edelstein SJ (2005) *Science* 308:1424–1428.
4. Lakey JH, Raggett EM (1998) *Curr Opin Struct Biol* 8:119–123.
5. Cooper MA (2003) *Anal Bioanal Chem* 377:834–842.
6. Piehler J (2005) *Curr Opin Struct Biol* 15:4–14.
7. Carrion-Vazquez M, Oberhauser AF, Fisher TE, Marszalek PE, Li H, Fernandez JM (2000) *Prog Biophys Mol Biol* 74:63–91.
8. Lu H, Schulten K (2000) *Biophys J* 79:51–65.
9. Paci E, Karplus M (2000) *Proc Natl Acad Sci USA* 97:6521–6526.
10. Ainavarapu SR, Li L, Badilla CL, Fernandez JM (2005) *Biophys J* 89:3337–3344.
11. Li H, Carrion-Vazquez M, Oberhauser AF, Marszalek PE, Fernandez JM (2000) *Nat Struct Biol* 7:1117–1120.
12. Rief M, Gautel M, Oesterhelt F, Fernandez JM, Gaub HE (1997) *Science* 276:1109–1112.
13. Akerstrom B, Brodin T, Reis K, Bjorck L (1985) *J Immunol* 135:2589–2592.
14. Nilson B, Bjorck L, Akerstrom B (1986) *J Immunol Methods* 91:275–281.
15. Sloan DJ, Hellinga HW (1999) *Protein Sci* 8:1643–1648.
16. Sagawa T, Oda M, Morii H, Takizawa H, Kozono H, Azuma T (2005) *Mol Immunol* 42:9–18.
17. Li Q, Du HN, Hu HY (2003) *Biopolymers* 72:116–122.
18. Powell KD, Ghaemmaghami S, Wang MZ, Ma L, Oas TG, Fitzgerald MC (2002) *J Am Chem Soc* 124:10256–10257.
19. Sjobring U, Bjorck L, Kastern W (1991) *J Biol Chem* 266:399–405.
20. Sauer-Eriksson AE, Kleywegt GJ, Uhlen M, Jones TA (1995) *Structure (London)* 3:265–278.
21. Cao Y, Lam C, Wang M, Li H (2006) *Angew Chem Int Ed Engl* 45:642–645.
22. Cao Y, Li H (2007) *Nat Mater* 6:109–114.
23. Li PC, Makarov DE (2004) *J Phys Chem B* 108:745–749.
24. Nauli S, Kuhlman B, Baker D (2001) *Nat Struct Biol* 8:602–605.
25. Marko JF, Siggia ED (1995) *Macromolecules* 28:8759–8770.
26. Hann E, Kirkpatrick N, Kleanthous C, Smith DA, Radford SE, Brockwell DJ (2007) *Biophys J* 92:L79–L81.
27. Junker JP, Hell K, Schlierf M, Neupert W, Rief M (2005) *Biophys J* 89:L46–L48.
28. Ha T, Zhuang X, Kim HD, Orr JW, Williamson JR, Chu S (1999) *Proc Natl Acad Sci USA* 96:9077–9082.
29. Majumdar DS, Smirnova I, Kasho V, Nir E, Kong X, Weiss S, Kaback HR (2007) *Proc Natl Acad Sci USA* 104:12640–12645.
30. Florin EL, Moy VT, Gaub HE (1994) *Science* 264:415–417.
31. Akerstrom B, Bjorck L (1986) *J Biol Chem* 261:10240–10247.
32. Gulich S, Linhult M, Stahl S, Hober S (2002) *Protein Eng* 15:835–842.
33. Malakauskas SM, Mayo SL (1998) *Nat Struct Biol* 5:470–475.
34. Saha K, Bender F, Gizeli E (2003) *Anal Chem* 75:835–842.
35. Walker KN, Bottomley SP, Popplewell AG, Sutton BJ, Gore MG (1995) *Biochem J* 310:177–184.
36. Marko JF, Siggia ED (1997) *Biophys J* 73:2173–2178.
37. Segel IH (1993) *Enzyme Kinetics* (Wiley, New York).